Tepljakov, Aleksei; González, Emmanuel A.; Petlenkov, Eduard; Belikov, Juri; Monje, Concepción A.; Petráš, Ivo (2016). Incorporation of fractional-order dynamics into an existing PI/PID DC motor control loop, *ISA Transactions*, v. 60, pp.: 262-273.

DOI: https://doi.org/10.1016/j.isatra.2015.11.012

Incorporation of Fractional-Order Dynamics into an Existing PI/PID DC Motor Control Loop

Aleksei Tepljakov[a,*], Emmanuel A. Gonzalez[b], Eduard Petlenkov[a], Juri Belikov[c], Concepción A. Monje[d], Ivo Petráš[e]

[a] *Department of Computer Control, Tallinn University of Technology, Ehitajate tee 5, 19086 Tallinn, Estonia, Fax (+372) 620 2101*
[b] *Existing Installation Department, Jardine Schindler Elevator Corporation, 8/F Pacific Star Bldg., Sen. Gil Puyat Ave. cor. Makati Ave., Makati City, 1209 Philippines*
[c] *Institute of Cybernetics, Tallinn University of Technology, Akadeemia tee 21, 12618 Tallinn, Estonia*
[d] *Systems Engineering and Automation Department, University Carlos III of Madrid, 28911 Leganés Madrid, Spain*
[e] *Institute of Control and Informatization of Production Processes, Faculty BERG, Technical University of Košice, B. Nemcovej 3, 042 00 Košice, Slovakia*

Abstract

The problem of changing the dynamics of an existing DC motor control system without the need of making internal changes is considered in the paper. In particular, this paper presents a method for incorporating fractional-order dynamics in an existing DC motor control system with internal PI or PID controller, through the addition of an external controller into the system and by tapping its original input and output signals. Experimental results based on the control of a real test plant from MATLAB/Simulink environment are presented, indicating the validity of the proposed approach.

Keywords: Fractional calculus; Fractional PID control; SISO control; Process control; Controller tuning; DC motor; Servo system

1. Introduction

Fractional calculus offers novel modeling tools for the analysis of dynamical systems. In particular, memory-like, hereditary, or self-similarity phenomena arising in

*Corresponding author

Email addresses: aleksei.tepljakov@ttu.ee (Aleksei Tepljakov), emm.gonzalez@delasalle.ph (Emmanuel A. Gonzalez), eduard.petlenkov@ttu.ee (Eduard Petlenkov), jbelikov@cc.ioc.ee (Juri Belikov), cmonje@ing.uc3m.es (Concepción A. Monje), ivo.petras@tuke.sk (Ivo Petráš)

physical systems are better described by models based on noninteger differential equations [1, 2]. In control engineering fractional process models have been proposed and successfully applied to describe certain systems [3, 4]. The fractional-order PID controller has been proposed in [5] and further studied in [6]. Such a controller has more tuning freedom and a wider region of parameters that may stabilize the plant under control. It has been confirmed that fractional-order PID controllers offer superior performance than their integer-order counterparts; in particular, in application to servo system control [7, 8, 9]. Tuning methods for FOPID controllers were presented in, e.g., [8, 10, 11, 12, 13, 14].

It is a known fact that the majority of industrial control loops are of PI/PID type [15]. It is therefore of significant interest to study the problem of enhancing conventional PID controllers by introducing additional dynamical properties arising from making use of fractional-order integrators and differentiators. However, introducing changes into existing control loops may require termination of an industrial process and thereby potentially result in production losses. Integrating a fractional-order controller into a working loop in a non intrusive way is therefore beneficial, and forms the main motivation of the present paper.

In this work, the following problem is addressed. A DC motor control system is considered described by a conventional first-order plus dead time (FOPDT) plant represented by $P(s)$ and having the general form

$$P(s) = \frac{K_m}{sT_m + 1}\mathrm{e}^{-L_m s}, \tag{1}$$

where it is assumed without loss of generality that $K_m, L_m, T_m > 0$, and a controller represented by $C(s)$ which could either be a classical proportional-integral (PI)

$$C_{PI}(s) = K_P + \frac{K_I}{s}, \tag{2}$$

or proportional-integral-derivative (PID) controller

$$C_{PID}(s) = K_P + \frac{K_I}{s} + K_D s, \tag{3}$$

where $K_P, K_I, K_D > 0$ are also assumed within a unity-feedback system. By combining the plant (1) and one of the controllers in (2) or (3), it can be seen that step and frequency responses will follow integer-order dynamics since the resulting denominator polynomial of the total transfer functions is governed by an integer-order polynomial.

The objective of the control algorithm proposed in this paper is to change the dynamics of the entire DC motor control system by incorporating fractional-order dynamics and eliminating the original influence of the classical PI or PID controllers, without making internal changes into the system. In particular, the objective is to make the entire system follow certain fractional-order dynamics. The latter can be achieved by using a fractional-order PID (FOPID) controller designed subject to particular specifications.

The contribution of this paper is as follows. First, the proposed retuning algorithm is described. Next, the design of a suitable FOPI or FOPID controller for an industrial process is detailed. The complete algorithm is then applied to a real-life model of an industrial object—a modular servo system—thereby indicating the validity of the proposed method through real-time experiments.

The novelty of the paper lies in experimental verification of the retuning method thereby expanding the results achieved only through simulations in [16]. Similar practical results are not known from prior art. Our earlier contribution [17] focuses on a different application of the retuning algorithm for a different type of plant. In this work, the choice of the experimental setup is based on the finding [7] that fractional-order controllers provide superior control characteristics compared to conventional ones in case of servo control.

The structure of the paper is as follows. In Section 2 the reader is introduced to basic concepts of fractional-order modeling. The proposed control architecture and tuning algorithm are detailed in Section 3. The description of the real-life servo system is given in Section 4, where, in addition, the dynamic model of the velocity control process is identified, and conventional PI and PID controllers are designed following a set of classical tuning rules. The application of the retuning method is illustrated in Section 5. Finally, conclusions are drawn in Section 6.

2. Brief Introduction to Fractional-order Modeling and Control

Fractional calculus is a generalization of integration and differentiation to the non-integer order operator ${}_a\mathscr{D}_t^\alpha$, where a and t denote the limits of the operation [8]. The continuous integro-differential operator of order $\alpha \in \mathbb{R}$ is defined in the following way

$$
{}_a\mathscr{D}_t^\alpha = \begin{cases} \mathrm{d}^\alpha/\mathrm{d}t^\alpha & \alpha > 0, \\ 1 & \alpha = 0, \\ \int_a^t (\mathrm{d}\tau)^{-\alpha} & \alpha < 0. \end{cases} \tag{4}
$$

In this paper we consider Caputo's definition of the fractional operator which is given by

$$
{}_0^C\mathscr{D}_t^\alpha f(t) = \frac{1}{\Gamma(m-\alpha)} \int_0^t \frac{f^{(m)}(\tau)}{(t-\tau)^{\alpha-m+1}} \mathrm{d}\tau, \tag{5}
$$

where $m - 1 < \alpha < m, m \in \mathbb{N}$, $\alpha \in \mathbb{R}_+$. The reason for adopting this definition is the practical applicability thereof, since it offers physically coherent meaning of initial conditions when solving corresponding fractional differential equations [1].

Assuming zero initial conditions, the Laplace transform of the fractional derivative in (5) is given by

$$
\int_0^\infty \mathrm{e}^{-st} {}_0\mathscr{D}_t^\alpha f(t) \mathrm{d}t = s^\alpha F(s). \tag{6}
$$

Thus, a fractional-order transfer function with a delay may be considered in the s-domain such that

$$
G(s) = \frac{b_m s^{\beta_m} + b_{m-1} s^{\beta_{m-1}} + \cdots + b_0 s^{\beta_0}}{a_n s^{\alpha_n} + a_{n-1} s^{\alpha_{n-1}} + \cdots + a_0 s^{\alpha_0}} \mathrm{e}^{-Ls}, \tag{7}
$$

where it is usual to take $\beta_0 = \alpha_0 = 0$, in which case the static gain of the system is given by $K = b_0/a_0$.

In real-life applications approximations of fractional-order operators are often used. In this work, Oustaloup's approximation method is considered. It is described in [18]. The method allows one to obtain a band-limited approximation of a fractional-order differentiator or integrator in the form $s^\alpha \approx H(s)$, where $\alpha \in (-1, 1) \subset \mathbb{R}$ and $H(s)$ is a conventional continuous-time linear system. The following approximation parameters are considered: filter order N such that the resulting integer-order model order is $2N+1$, and frequency band limits (ω_b, ω_h). The continuous-time representation can be used for digital filter implementation by applying a proper discretization method [19].

3. New Control Architecture and Tuning Algorithm

Consider an ordinary unity-feedback control system consisting of a controller $C(s)$ and plant $P(s)$. The controller $C(s)$ is assumed to be either of PI or PID type tuned to stabilize the plant. The feedback control system therefore follows the rules of integer-order differential equations. The objective is to plug in an external fractional-order controller $C_R(s)$ into the existing control system in such a way that the dynamics of the overall system follows the rules governed by fractional-order differential equations. The control architecture with an external controller incorporated into an existing feedback control system is shown in Fig. 1. The results of this paper are partially based on results in [20], where a retuning method for a conventional integer-order PI/PID was studied. The extension of these results for FO controllers brings about a considerable amount of benefit due to additional tuning flexibility and the ability to satisfy more design specifications such as the often desired iso-damping property of the control loop. The external fractional-order controller $C_R(s)$ captures the input and output signals of the original feedback control system and feeds a corrective signal in addition to the input signal into the feedback control system [16, 21]. The effect of a double feedback configuration in Fig. 1 is equivalent to a simple unity-gain feedback control system with the controller

$$C^*(s) \quad = \quad (C_R(s) + 1)\, C(s) \tag{8}$$

as shown in Fig. 2.

3.1. Retuning Control Architecture

Let us consider the FOPDT plant in (1). In what follows, several propositions related to the suggested control system retuning architecture are provided.

Proposition 1 (from PI to PI$^\lambda$)**.** *Consider the original integer-order PI controller in* (2)*. Let $C_{R1}(s)$ be a controller of the form*

$$C_{R1}\,(s) = \frac{K_1 s^\alpha + (K_0 - K_P)\, s - K_I}{K_P s + K_I}, \tag{9}$$

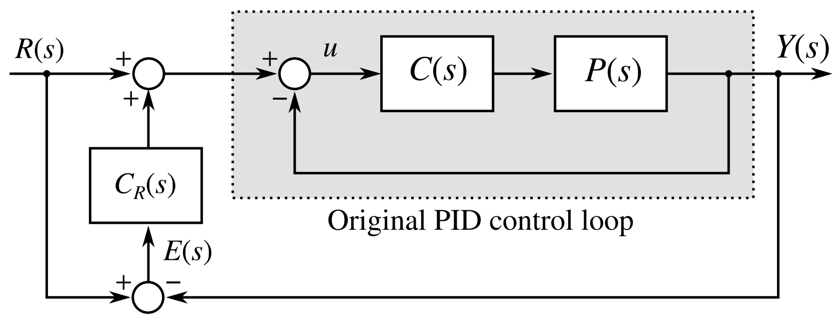

Figure 1: The retuning architecture where an external controller $C_R(s)$ is added into the system without compromising the internal connection of the original closed-loop system

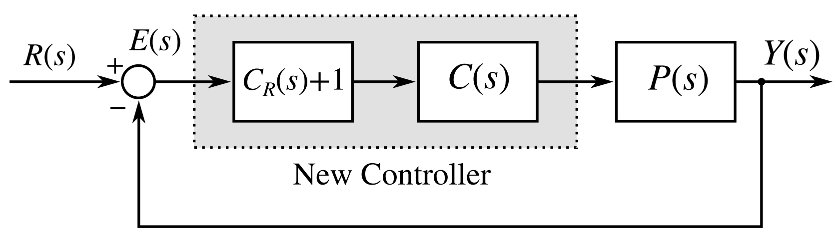

Figure 2: Equivalent architecture of Fig. 1 after application of block diagram algebra. The combination of $C_R(s)$ and $C(s)$ results in an equivalent controller $C^*(s)$ as described in Eq. (8)

where the coefficients are $K_P, K_I, K_1, K_0 > 0$ and the order is $-1 < \alpha < 1$. The resulting PI$^\lambda$ controller from a classical PI controller with parameters $K_P, K_I > 0$ has the following coefficients:

$$K_P^* = K_0, \tag{10}$$

and

$$K_I^* = K_1. \tag{11}$$

The order of fractional-order integration is

$$\lambda = 1 - \alpha. \tag{12}$$

Proof. Incorporating (2) and (9) into (8) yields

$$\begin{aligned} C^*(s) &= \left(C_{R1}(s) + 1\right) C(s) \\ &= \frac{K_1 s^\alpha + \left(K_0 - K_P\right) s - K_I + K_P s + K_I}{K_P s + K_I} \left(\frac{K_P s + K_I}{s}\right) \\ &= K_0 + \frac{K_1}{s^{1-\alpha}} = K_P^* + \frac{K_I^*}{s^\lambda}. \end{aligned} \tag{13}$$

Therefore, it can be seen from (13) that (10), (11), and (12) hold true [16]. ■

Proposition 2 (from PI to PI$^\lambda$D$^\mu$)**.** *Consider the original integer-order PI controller in* (2)*. Let $C_{R2}(s)$ be a controller of the form*

$$C_{R2}\left(s\right) = \frac{K_2 s^\beta + K_1 s^\alpha + \left(K_0 - K_P\right) s - K_I}{K_P s + K_I}, \tag{14}$$

where the coefficients are $K_P, K_I, K_2, K_1, K_0 > 0$, and the orders are $-1 < \alpha < 1$ and $1 < \beta < 2$. The resulting PI$^\lambda$D$^\mu$ controller from a classical PI controller with parameters $K_P, K_I > 0$ has the following coefficients:

$$K_P^* = K_0, \tag{15}$$

$$K_I^* = K_1, \tag{16}$$

and

$$K_D^* = K_2. \tag{17}$$

The order of fractional-order integration is

$$\lambda = 1 - \alpha, \tag{18}$$

while fractional-order differentiation is

$$\mu = \beta - 1. \tag{19}$$

Proof. Incorporating (2) and (14) into (8) yields

$$\begin{aligned} C^*(s) &= \left(C_{R2}(s)+1\right)C(s) \\ &= \frac{1}{K_P s + K_I} \times \big(K_2 s^{\beta} + K_1 s^{\alpha} + (K_0 - K_P)\, s - K_I \\ &\quad + K_P s + K_I\big)\left(\frac{K_P s + K_I}{s}\right) \\ &= K_0 + \frac{K_1}{s^{1-\alpha}} + K_2 s^{\beta - 1} = K_P^* + \frac{K_I^*}{s^{\lambda}} + K_D^* s^{\mu}. \end{aligned} \tag{20}$$

Therefore, it can be seen from (20) that (15), (16), (17), (18), and (19) hold true [16].

■

Proposition 3 (from PID to PI$^{\lambda}$D$^{\mu}$)**.** *Consider the original integer-order PID controller in* (3)*. Let $C_{R3}(s)$ be a controller of the form*

$$C_{R3}(s) = \frac{K_2 s^{\beta} + K_1 s^{\alpha} - K_D s^2 + (K_0 - K_P)\, s - K_I}{K_D s^2 + K_P s + K_I}, \tag{21}$$

where the coefficients are $K_P, K_I, K_D, K_2, K_1, K_0 > 0$, and the orders are $-1 < \alpha < 1$ and $1 < \beta < 2$. The resulting PI$^{\lambda}$D$^{\mu}$ controller from a classical PID controller with parameters $K_P, K_I, K_D > 0$ has the following coefficients:

$$K_P^* = K_0, \tag{22}$$

$$K_I^* = K_1, \tag{23}$$

and

$$K_D^* = K_2. \tag{24}$$

The order of fractional-order integration is

$$\lambda = 1 - \alpha, \tag{25}$$

while fractional-order differentiation is

$$\mu = \beta - 1. \tag{26}$$

Proof. Incorporating (3) and (21) into (8) yields

$$\begin{aligned}
C^*(s) &= (C_{R3}(s)+1)\,C(s) \\
&= \frac{1}{K_D s^2 + K_P s + K_I} \\
&\quad \times \left(K_2 s^\beta + K_1 s^\alpha - K_D s^2 + (K_0 - K_P)\,s - K_I\right. \\
&\quad \left. + K_P s + K_I\right)\left(\frac{K_D s^2 + K_P s + K_I}{s}\right) \\
&= K_0 + \frac{K_1}{s^{1-\alpha}} + K_2 s^{\beta-1} = K_P^* + \frac{K_I^*}{s^\lambda} + K_D^* s^\mu. \qquad (27)
\end{aligned}$$

Therefore, it can be seen from (27) that (22), (23), (24), (25), and (26) hold true [16].

■

In what follows, the retuning algorithm is summarized and the details pertaining to the design of suitable FOPI/FOPID controllers are provided.

3.2. Summary of the Retuning Algorithm

1. **Identify the type of fractional-order controller to be used, i.e., PI$^\lambda$ or PI$^\lambda$D$^\mu$, based on the desired control requirements.** The choice of whether a PI$^\lambda$ or PI$^\lambda$D$^\mu$ controller shall be used depends on the number and types of criteria to be satisfied and the model of the plant. Discussion on the different types of robustness criteria such as phase margin and gain crossover frequency specifications, robustness to gain variations (iso-damping property), low-frequency noise and good output disturbance rejection are presented in [8].
2. **Solve for the coefficients of the overall controller $C^*(s)$ using any method based on the plant's model and robustness criteria to be satisfied.** For robustness, tuning methods for PI$^\lambda$ controllers can be found in [13, 22, 23], while methods for tuning PI$^\lambda$D$^\mu$ controller can be found in [24, 25]. The description of the toolset used to design a suitable FOPID controller in the context of this work is provided in Subsection 3.3.
3. **Calculate the parameters of $C_R(s)$.** The formulas from Propositions 1–3 are as follows: Eqs. (10)–(12) for PI to PI$^\lambda$ retuning, Eqs. (15)–(19) for PI to PI$^\lambda$D$^\mu$ retuning, and Eqs. (22)–(26) for PID to PI$^\lambda$D$^\mu$ retuning.

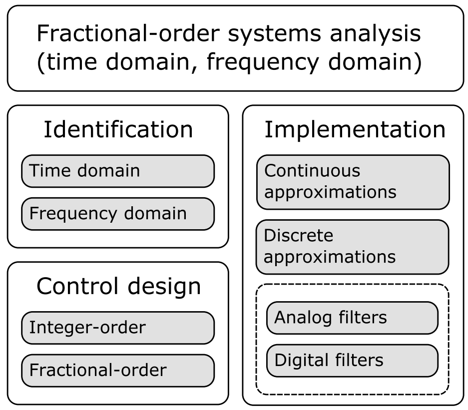

Figure 3: FOMCON toolbox structure

3.3. FOPID Controller Design

In this work, for the purpose of controller design FOMCON ("Fractional-order Modeling and Control") toolbox for MATLAB/Simulink is used [26, 27]. In the following, a brief description of the FOMCON toolbox and the modules thereof that are applied in this work is provided.

The structure of the toolbox is given in Fig. 3. There are currently four main modules: the main system analysis module (toolbox core), system identification module, control design module and fractional-order system implementation module. The focus is on the following particular tools:

- Time domain identification;
- Fractional-order control design based on constrained optimization.

The time-domain identification module allows one to obtain generalized models of the studied process or system in the form (7). Therefore, one can also use it to identify conventional models, such as the FOPDT model in (1).

Having acquired a model using the identification module, the FOPID optimization tool can be applied for accomplishing the task of model-based control design. The tool itself was inspired by [8, 28] and is thoroughly described in [14, 29].

The general procedure of FOPID controller design may be summarized by the following steps:

- Depending on the plant characteristics, determine the correct frequency range for approximation. Oustaloup filters are always used due to their flexibility [8].
- Obtain an initial feasible parameter set for the fractional-order PID controller;
- Choose controller gain/exponent constraints by taking the dynamical characteristics of the plant into account;
- Choose control system constraints based on frequency domain analysis of the open loop;
- Decide whether you want to use Simulink for system simulation, and if so, specify the correct control saturation values of the actuator.

Next, the choice of an appropriate performance metric is required (four are provided: ISE, IAE, ITSE, and ITAE). The selection of this parameter depends on the desired dynamical properties of the control loop [30]. Limiting the number of iterations can help determine whether the initial parameter selection can ultimately lead to a feasible result.

In this work, the following control system design specifications are considered:

- Phase margin φ_m and the corresponding crossover frequency ω_c;
- Robustness to gain variations [31], which requires the phase response of the open loop control system to be flat at ω_c, i.e.,

$$\frac{\mathrm{d}}{\mathrm{d}\omega}(\arg C(j\omega)P(j\omega))\bigg|_{\omega=\omega_c} = 0. \tag{28}$$

This section is concluded by stressing the importance of the actuator saturation problem in real-life systems. From the point of view of linear system theory, frequency-domain specifications given above are only valid when the closed-loop control system operates without control law saturation. However, achieving a system without saturation by limiting controller gains is not favorable since it may reduce set-point tracking performance and, in general, contradicts the goals of optimal control [32]. Hence, the authors of this work allow actuator saturation in the context of the given problem, but verify the performance of the resulting control system.

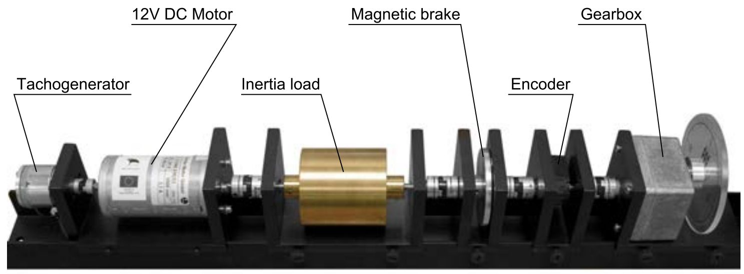

Figure 4: The INTECO DC motor platform used for the experiments

4. DC Motor Platform Experimental Setup

In this work, the following particular configuration of the INTECO modular servo system [33] is considered as shown in Fig. 4, in which the objective is to control the angular velocity of the DC motor. This modular experimental platform consists of the following components: a tachogenerator, a 24V DC motor, an inertia load, a magnetic brake, an encoder, and a gearbox. The servo system may be interfaced with the MATLAB/Simulink environment through a specific PCI board, where data is collected from the encoder and tachogenerator, and is sent to the power drive box, which controls the DC motor.

In order to identify the model of the system, one may use the FOMCON identification tool. As a result, a conventional FOPDT model is obtained, i.e., the power α in s^α is close to one. In addition, the time delay is found to be insignificant. The following model was identified:

$$P(s) = \frac{166.3714}{0.83907s + 1}. \tag{29}$$

This model is used in all subsequent system simulations. A special model was also fitted to the response with an experimentally set time delay of 0.1 seconds resulting in

$$P(s) = \frac{166.1038}{0.75507s + 1}\mathrm{e}^{-0.1s}. \tag{30}$$

The reason for doing this is the following. The addition of the delay term is necessary in order to enable the computation of the conventional and fractional-order PI and PID controllers. Further discussion in relation to the system's mathematical model identification is presented in [34].

The original feedback control system is in the form of a unity-feedback system, where the controller is either PI or a PID controller. The parameters of the original PI and PID controllers will be used as part of the retuning process, which is illustrated in the examples found in Section 5. Initially it is assumed that the existing PI and PID controller design is based on Ziegler-Nichols tuning method [35]. The rationale behind choosing this particular method is that it is one of the most popular methods for tuning industrial PID control loops [15]. Therefore, it is expected that a lot of existing loops have already been tuned according to this method. Obviously it is possible to obtain a much better result by studying each particular control problem in detail and applying, e.g., optimization based control design techniques even with classical PID controllers. However, in the context of this work these particular techniques are extended to satisfy more design specifications by means of using FOPID controllers. Hence it is natural to assume that using the FOPID retuning method with existing PID control loops tuned according to conventional rules such as the Ziegler-Nichols method will result in significant improvement of control quality and performance.

The tuning method of classical PI (2), and PID (3) controllers for a FOPDT system with quarter-decay ratio $L_m/T_m \leq 1$, as detailed in [36, pp. 30, 78], is as follows: $K_P = 0.9T_m/(K_m L_m) = 0.0409$ and $K_I = T/(3.7K_m L_m^2) = 0.1229$ for classical PI, and $K_P = 2T_m/(K_m L_m) = 0.0909$, $K_I = T/(K_m L_m^2) = 0.4546$ and $K_D = T_m/K_m = 0.0045$ for classical PID. The numerically simulated step responses and control signals for (29) with classical PI and PID controllers are shown in Figs. 5 and 6, while the actual experimental step responses and control signals are shown in Figs. 7 and 8. These two figures each present three responses considering that the motor system parameter K_m is a varying parameter with a tolerance of $\pm 25\%$, resulting in the range $K_m \in [124.7786, 207.9642]$. Such setup was made to show the effectiveness of the fractional-order controllers on robustness applications in the next section.

From Figs. 7 and 8, one can see that the damping property of the entire feedback control system is not uniform, i.e., the step response overshoots vary with large amounts from around 120 rad/s to around 150 rad/s, with a step command of 100 rad/s. The classical PI and PID controllers were not able to address this type of situation as evidently shown in open-loop frequency responses in Figs. 9 and 10, in which the

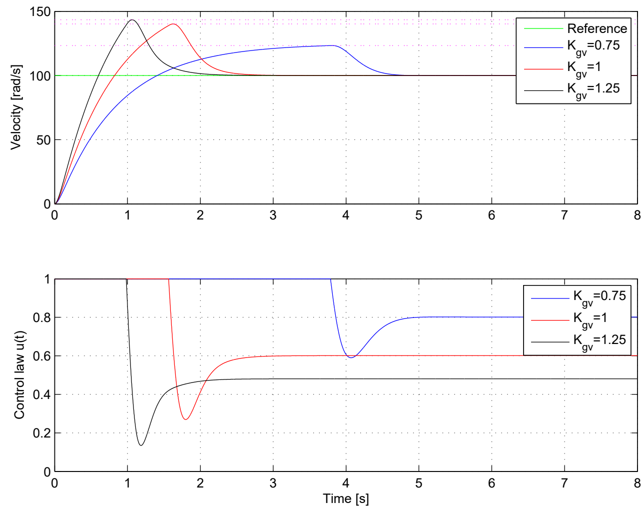

Figure 5: Simulated step responses and control signals of the original feedback control system with a classical PI controller. Experimentation was done with $0.75K_m$, $1.0K_m$, and $1.25K_m$ as numerator parameters of (29)

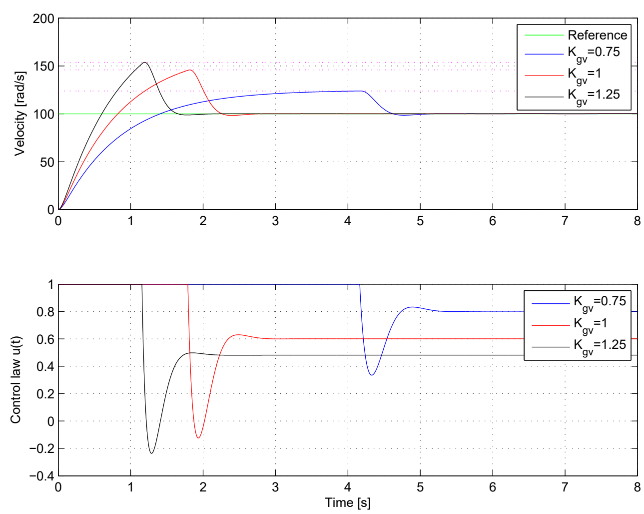

Figure 6: Simulated step responses and control signals of the original feedback control system with a classical PID controller. Experimentation was done with $0.75K_m$, $1.0K_m$, and $1.25K_m$ as numerator parameters of (29)

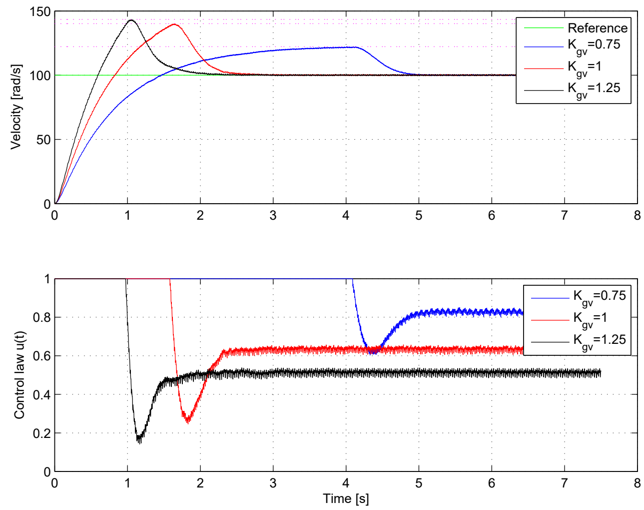

Figure 7: Hardware experimentation step responses and control signals of the original feedback control system with a classical PI controller. Experimentation was done with $0.75K_m$, $1.0K_m$, and $1.25K_m$ as numerator parameters of (29)

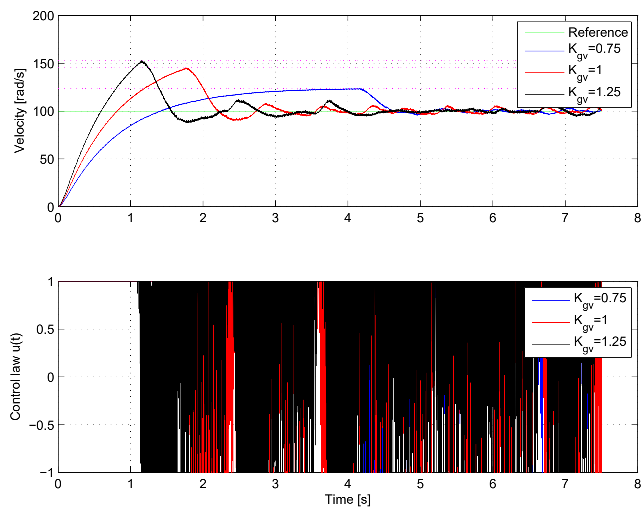

Figure 8: Hardware experimentation step responses and control signals of the original feedback control system with a classical PID controller. Experimentation was done with $0.75K_m$, $1.0K_m$, and $1.25K_m$ as numerator parameters of (29)

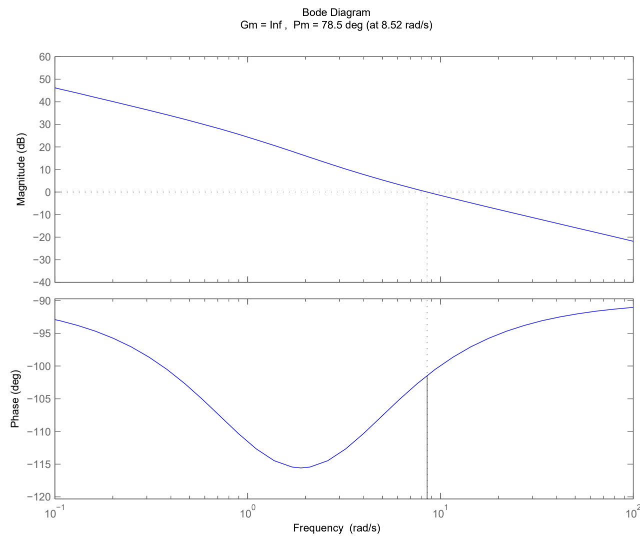

Figure 9: Open-loop frequency response of the original feedback control system with a classical PI controller and plant gain of $1.0K_m$

rate-of-change of the phase value at the cross-over frequency is not zero; that is, the requirement in (28) is not satisfied. In case of the PID controller, one can also observe rapid control law oscillations due to the derivative component gain. This is not acceptable in a real application.

5. Experimental Retuning Results

For the retuning examples, the following PI$^\lambda$ controller is considered

$$C^*_{FOPI}(s) = 0.054972 + \frac{0.055043}{s^{0.6631}} \tag{31}$$

with the specifications $\varphi_m = 87$ and $\omega_{cg} = 12$ rad/s, and the PI$^\lambda$D$^\mu$ controller

$$C^*_{FOPID}(s) = 0.005 + \frac{0.021235}{s^{0.8}} + 0.0014588 s^{0.5} \tag{32}$$

with the specifications $\varphi_m = 97.3°$ and $\omega_{cg} = 2.5$ rad/s. The controllers were obtained using the method described in Section 3.3 with the model in (29) taken as basis for model-based design. The tuning is accomplished offline, and the difference in design specifications—phase margin and crossover frequency—arises from the desire to obtain particular nominal step responses in each case.

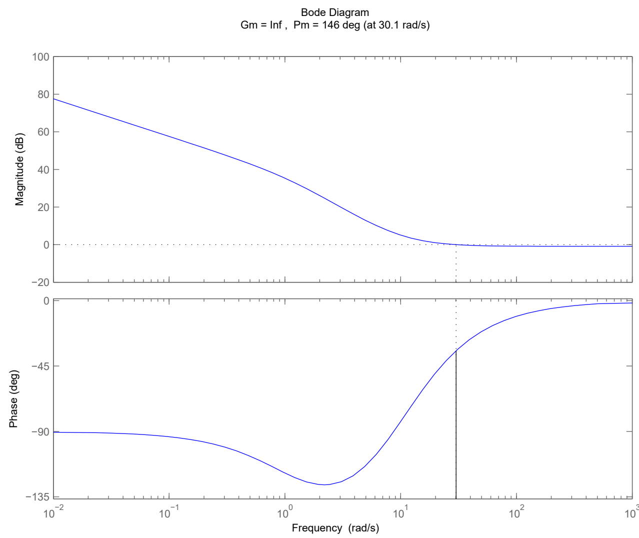

Figure 10: Open-loop frequency response of the original feedback control system with a classical PID controller and plant gain of $1.0K_m$

Figs. 11 and 12 present the simulated step responses of the system with the application of PI$^\lambda$ and PI$^\lambda$D$^\mu$ controllers, respectively. It can be seen that the iso-damping property of the system is valid given that the variation of overshoots of the step responses is reasonably small. In fact, this variation coincides with corresponding linear simulations without modeling the actuator saturation effect. From frequency domain analysis, the iso-damping property can be seen in the phase response which has a slope of zero at the phase margin, as shown in Figs. 13 and 14 for PI$^\lambda$ and PI$^\lambda$D$^\mu$ controllers, respectively.

5.1. Example 1: From PI to PI$^\lambda$

In this example, it is assumed that the PI$^\lambda$ controller to be incorporated has the form (31) with $K_P^* = 0.054972$, $K_I^* = 0.055043$, and $\lambda = 0.6631$. Evaluating (10)–(12) yields the values $K_0 = K_P^* = 0.054972$, $K_1 = K_I^* = 0.055043$, and $\alpha = 1 - \lambda = 0.3369$. From (9), the resulting external controller can now be determined

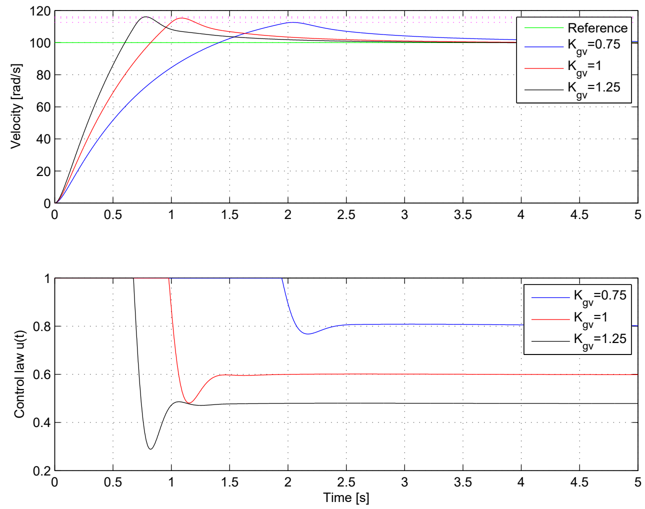

Figure 11: Simulated step responses and control signals of the original feedback control system with the PI$^{\lambda}$ controller. Experimentation was done with $0.75K_m$, $1.0K_m$, and $1.25K_m$ as numerator parameters of (29)

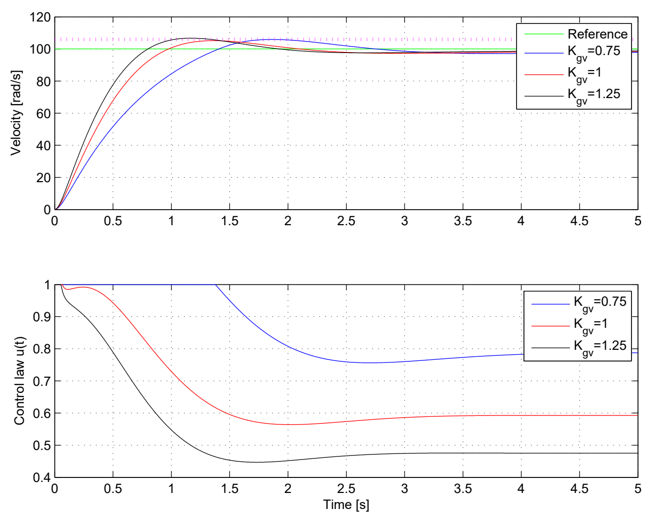

Figure 12: Simulated step responses and control signals of the original feedback control system with the PI$^{\lambda}$D$^{\mu}$ controller. Experimentation was done with $0.75K_m$, $1.0K_m$, and $1.25K_m$ as numerator parameters of (29)

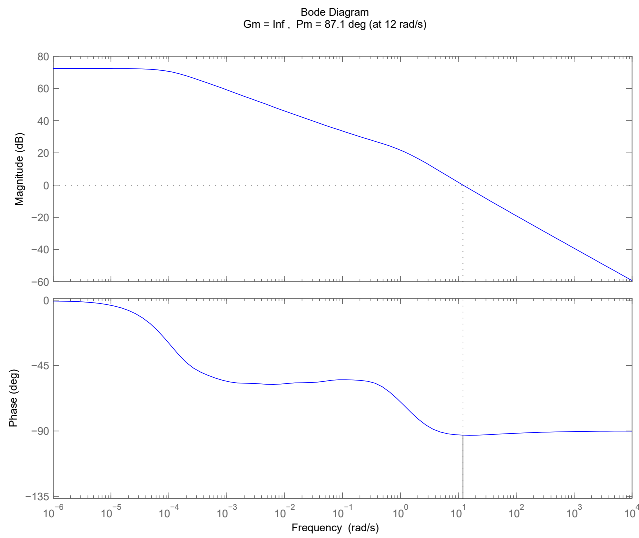

Figure 13: Open-loop frequency response of the original feedback control system with a PI$^\lambda$ controller and plant gain of $1.0K_m$

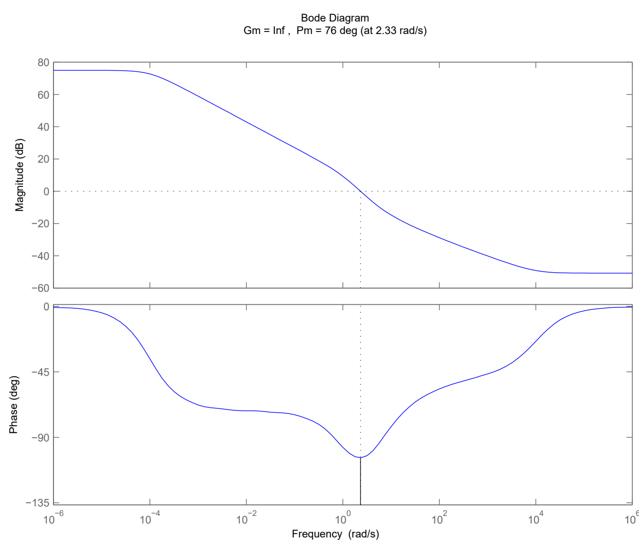

Figure 14: Open-loop frequency response of the original feedback control system with a PI$^\lambda$D$^\mu$controller and plant gain of $1.0K_m$

as

$$C_{R1}(s) = \frac{K_1 s^{\alpha} + (K_0 - K_P)\,s - K_I}{K_P s + K_I} = \frac{0.055043 s^{0.3369} + 0.028072 s - 0.055043}{0.0269 s + 0.055043}. \quad (33)$$

5.2. Example 2: From PI to PI$^{\lambda}$D$^{\mu}$

In this example, it is assumed that the PI$^{\lambda}D^{\mu}$ controller to be incorporated has the form (32) with $K_P^* = 0.005$, $K_I^* = 0.021235$, $K_D^* = 0.0014588$, $\lambda = 0.8$ and $\mu = 0.5$. Evaluating (15)–(19) yields the values $K_0 = K_P^* = 0.005$, $K_1 = K_I^* = 0.021235$, $K_2 = K_D^* = 0.0014588$, $\alpha = 1 - \lambda = 0.2$, and $\beta = \mu + 1 = 1.5$. From (14), the resulting external controller is the following one:

$$C_{R2}(s) = \frac{K_2 s^{\beta} + K_1 s^{\alpha} + (K_0 - K_P)\,s - K_I}{K_P s + K_I} = \frac{0.0014588 s^{1.5} + 0.21235 s^{0.2} - 0.0539 s - 0.1229}{0.0409 s + 0.1229}. \quad (34)$$

5.3. Example 3: From PID to PI$^{\lambda}$D$^{\mu}$

In this example, it is assumed that the PI$^{\lambda}D^{\mu}$ controller to be incorporated has the form (32) with $K_P^* = 0.005$, $K_I^* = 0.021235$, $K_D^* = 0.0014588$, $\lambda = 0.8$, and $\mu = 0.5$. Evaluating (22)–(26) yields the values $K_0 = K_P^* = 0.005$, $K_1 = K_I^* = 0.021235$, $K_2 = K_D^* = 0.0014588$, $\alpha = 1 - \lambda = 0.2$, and $\beta = \mu + 1 = 1.5$. From (21), the resulting external controller is the following one:

$$C_{R3}(s) = \frac{K_2 s^{\beta} + K_1 s^{\alpha} - K_D s^2 + (K_0 - K_P)\,s - K_I}{K_D s^2 + K_P s + K_I} = \frac{0.0014588 s^{1.5} + 0.21235 s^{0.2} - 0.0045 s^2 - 0.0859 s - 0.4546}{0.0045 s^2 + 0.0909 s + 0.4546}. \quad (35)$$

5.4. Retuning Algorithm Implementation and Real-Time Control Results

The algorithm is implemented in MATLAB/Simulink environment following the control architecture in Fig. 1. Oustaloup's recursive filter is used for realization of fractional-order controllers in (33)–(35). The following continuous-time approximations were obtained in MATLAB with $N = 5$, $\omega_b = 0.001$, and $\omega_h = 1000$:

$$\tilde{C}_{R1} = \frac{\tilde{C}_{R11}}{\tilde{C}_{R12}}, \quad \tilde{C}_{R2} = \frac{\tilde{C}_{R21}}{\tilde{C}_{R22}}, \quad \tilde{C}_{R3} = -\frac{\tilde{C}_{R31}}{\tilde{C}_{R32}}, \tag{36}$$

where

$$\begin{aligned} \tilde{C}_{R11} \quad = \quad & 0.34406(s+676.3)(s+196.4)(s+58.54)(s+17.86) \\ & \times(s+5.323)(s+1.48)(s+0.3988)(s+0.1086) \\ & \times(s+0.03002)(s+0.008387)(s+0.002356)(s-3.046), \end{aligned} \tag{37}$$

$$\begin{aligned} \tilde{C}_{R12} \quad = \quad & (s+659.4)(s+187.8)(s+53.49)(s+15.23) \\ & \times(s+4.338)(s+3.005)(s+1.236)(s+0.3519) \\ & \times(s+0.1002)(s+0.02854)(s+0.008129)(s+0.002315), \end{aligned} \tag{38}$$

and

$$\begin{aligned} \tilde{C}_{R21} \quad = \quad & 0.25015(s-1496)(s+604.9)(s+271.1)(s+172.1) \\ & \times(s+67.89)(s+48.88)(s+18.22)(s+13.76) \\ & \times(s+5.113)(s+1.32)(s+1.254)(s+0.3891) \\ & \times(s+0.3366)(s+0.111)(s+0.09463)(s+0.03162) \\ & \times(s+0.02675)(s+0.009006)(s+0.007578) \\ & \times(s+0.002565)(s+0.002148)(s^2+6.629s+11.11), \end{aligned} \tag{39}$$

$$\begin{aligned} \tilde{C}_{R22} \quad = \quad & (s+730.5)(s+605.1)(s+208.1)(s+172.3) \\ & \times(s+59.26)(s+49.08)(s+16.88)(s+13.98) \\ & \times(s+4.806)(s+3.981)(s+3.005)(s+1.369) \\ & \times(s+1.134)(s+0.3899)(s+0.3229)(s+0.111) \\ & \times(s+0.09197)(s+0.03162)(s+0.02619)(s+0.009006) \\ & \times(s+0.00746)(s+0.002565)(s+0.002125), \end{aligned} \tag{40}$$

and finally

$$
\begin{aligned}
\tilde{C}_{R31} = {} & (s+724.4)(s+605.1)(s+205.8)(s+172.4) \\
& \times(s+57.78)(s+49.17)(s+4.495)(s+4.225) \\
& \times(s+1.365)(s+1.151)(s+0.3897)(s+0.326) \\
& \times(s+0.111)(s+0.09262)(s+0.03162)(s+0.02633) \\
& \times(s+0.009006)(s+0.00749)(s+0.002565) \\
& \times(s+0.002131)(s^2+29.03s+214.3) \\
& \times(s^2+20.47s+110.9),
\end{aligned} \tag{41}
$$

$$
\begin{aligned}
\tilde{C}_{R32} = {} & (s+730.5)(s+605.1)(s+208.1)(s+172.3) \\
& \times(s+59.26)(s+49.08)(s+16.88)(s+13.98) \\
& \times(s+11.09)(s+9.106)(s+4.806)(s+3.981) \\
& \times(s+1.369)(s+1.134)(s+0.3899)(s+0.3229) \\
& \times(s+0.111)(s+0.09197)(s+0.03162) \\
& \times(s+0.02619)(s+0.009006)(s+0.00746) \\
& \times(s+0.002565)(s+0.002125).
\end{aligned} \tag{42}
$$

Experimental results obtained from the motor platform with the retuning controllers given above are shown in Figs. 15 and 16. PID control loop retuning ultimately leads to equivalent PI$^\lambda$ or PI$^\lambda$D$^\mu$ control loops, therefore only two sets of experiments are considered, as equivalent configurations generate results that are very similar.

6. Conclusions

In this paper, retuning heuristics were implemented with the objective of incorporating fractional-order dynamics in an existing integer-order DC feedback control system. It was shown that an external controller $C_R(s)$ could be designed, implemented and incorporated into the feedback control system by just obtaining the input and output signals without any changes in the configuration of the original DC motor system.

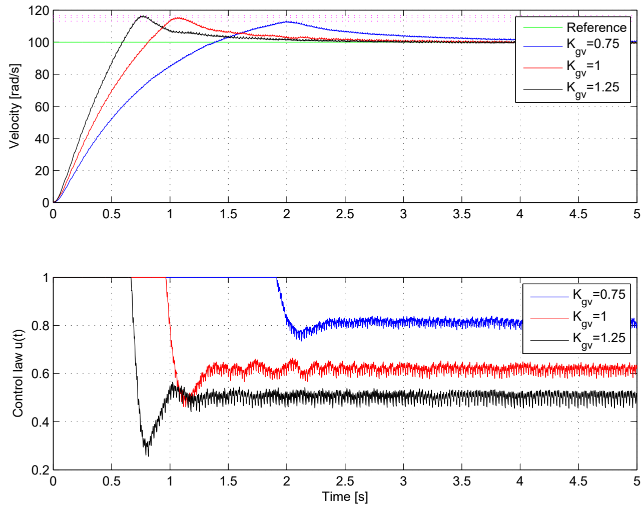

Figure 15: Experimental step responses and control signals of the original feedback control system with the PI$^\lambda$ controller with retuning controller C_{R1}. Experimentation was done with $0.75K_m$, $1.0K_m$ and $1.25K_m$ as numerator parameters of (29) on a DC motor system

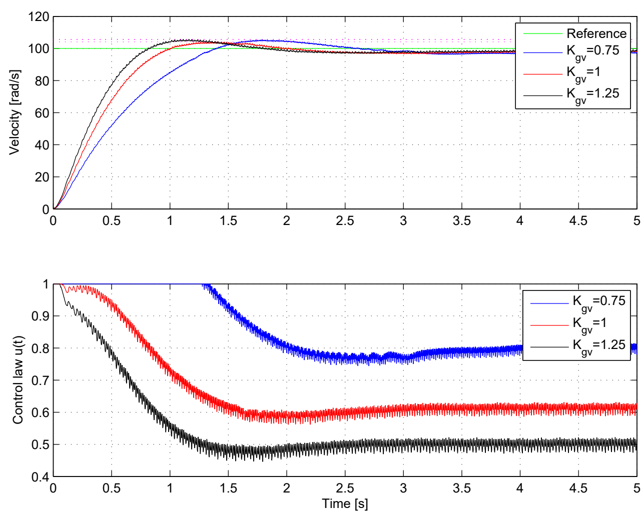

Figure 16: Experimental step responses and control signals of the original feedback control system with the PI$^\lambda$D$^\mu$ controller with retuning controllers C_{R2} and C_{R3}. Experimentation was done with $0.75K_m$, $1.0K_m$ and $1.25K_m$ as numerator parameters of (29) on a DC motor system

Both simulation and experimental results show that such retuning capability is possible in the essence of improving system's robustness, e.g., incorporating iso-damping property.

Future work will encompass further analysis of the retuning method with prospective industrial applications. The issue of efficient realization of the retuning controllers will also be studied.

Acknowledgment

This work was partially supported by the following grants under the Slovak Grant Agency, the Slovak Research and Development Agency: VEGA 1/0552/14, VEGA 1/0729/12, VEGA 1/0497/11, VEGA 1/2578/12, and APVV-0482-11, and the European Union through the European Regional Development Fund, and the Estonian Doctoral School in Information and Communication Technology through the interdisciplinary project FOMCON.

In Memoriam

The authors wish to thank Dr. L'ubomír Dorčák for his contributions to the manuscript. Dr. Dorčák passed away on July 14, 2014, and is dearly missed.

References

[1] I. Podlubny, Fractional differential equations, Mathematics in science and engineering, Academic Press, 1999.

[2] R. Hilfer, Applications of fractional calculus in physics, World Scientific, 2000.

[3] H. Malek, Y. Luo, Y. Q. Chen, Tuning fractional order proportional integral controllers for time delayed systems with a fractional pole, in: Proceedings of the ASME 2011 International Design Engineering Technical Conferences & Computers and Information in Engineering Conference, Vol. 3, 2011, pp. 1–11.

[4] A. Tepljakov, E. Petlenkov, J. Belikov, M. Halás, Design and implementation of fractional-order PID controllers for a fluid tank system, in: Proc. 2013 American Control Conference (ACC), Washington DC, USA, 2013, pp. 1780–1785.

[5] I. Podlubny, L. Dorčák, I. Kostial, On fractional derivatives, fractional-order dynamic systems and $\mathrm{PI}^{\lambda}\mathrm{D}^{\mu}$-controllers, in: Proc. 36th IEEE Conf. Decision and Control, Vol. 5, 1997, pp. 4985–4990. doi:10.1109/CDC.1997.649841.

[6] I. Podlubny, Fractional-order systems and $\mathrm{PI}^{\lambda}\mathrm{D}^{\mu}$-controllers, IEEE Transactions on Automatic Control 44 (1) (1999) 208–214. doi:10.1109/9.739144.

[7] D. Xue, C. Zhao, Y. Q. Chen, Fractional order PID control of a DC-motor with elastic shaft: a case study, in: Proc. 2006 American Control Conference (ACC), 2006.

[8] C. A. Monje, Y. Q. Chen, B. M. Vinagre, D. Xue, V. Feliu, Fractional-order Systems and Controls: Fundamentals and Applications, Advances in Industrial Control, Springer Verlag, 2010.

[9] S. H. HosseinNia, I. Tejado, B. M. Vinagre, Fractional-order reset control: Application to a servomotor, Mechatronics 23 (7) (2013) 781–788.

[10] S. E. Hamamci, An algorithm for stabilization of fractional-order time delay systems using fractional-order PID controllers., IEEE Transactions on Automatic Control 52 (10) (2007) 1964–1969.

[11] S. E. Hamamci, Stabilization using fractional-order PI and PID controllers, Nonlinear Dynamics 51 (1-2) (2008) 329–343.

[12] S. H. HosseinNia, I. Tejado, B. M. Vinagre, A method for the design of robust controllers ensuring the quadratic stability for switching systems, Journal of Vibration and Control (2012) 1–14.

[13] Y. Luo, Y. Q. Chen, Stabilizing and robust fractional order PI controller synthesis for first order plus time delay systems, Automatica 48 (9) (2012) 2159–2167.

[14] A. Tepljakov, E. Petlenkov, J. Belikov, A flexible MATLAB tool for optimal fractional-order PID controller design subject to specifications, in: W. Li, Q. Zhao (Eds.), Proc. the 31st Chinese Control Conference, Hefei, Anhui, China, 2012, pp. 4698–4703.

[15] K. Åström, T. Hägglund, Advanced PID control, The Instrumentation, Systems, and Automation Society (ISA), 2006.

[16] E. A. Gonzalez, C. A. Monje, L. Dorčák, J. Terpák, I. Petráš, A method for incorporating fractional-order dynamics through PID control system retuning, International Journal of Pure and Applied Mathematics 68 (4) (2013) 593–605.

[17] A. Tepljakov, E. Petlenkov, J. Belikov, E. A. Gonzalez, Design of retuning fractional PID controllers for a closed-loop magnetic levitation control system, in: ICARCV 2014 : The 13th International Conference on Control, Automation, Robotics & Vision, 2014, pp. 1345–1350.

[18] A. Oustaloup, F. Levron, B. Mathieu, F. M. Nanot, Frequency-band complex noninteger differentiator: characterization and synthesis, IEEE Transactions on Circuits and Systems—Part I: Fundamental Theory and Applications 47 (1) (2000) 25–39. doi:10.1109/81.817385.

[19] A. Tepljakov, E. Petlenkov, J. Belikov, Embedded system implementation of digital fractional filter approximations for control applications, in: Proc. 21st Int Mixed Design of Integrated Circuits and Systems (MIXDES) Conference, 2014.

[20] H. M. Son, Retuning of PI/PID controllers based on closed-loop model, in: The AUN/SEED-Net Fieldwise Seminar on Control Engineering, Montien Hotel, Bangkok Thailand, 2006.

[21] L. Dorčák, I. Petráš, E. A. Gonzalez, J. Valsa, J. Terpák, M. Zecova, Application of PID retuning method for laboratory feedback control system incorporating FO dynamics, in: Proc. of the 14th International Carpathian Control Conference (ICCC), 2013, pp. 38–43.

[22] C. Wang, Y. Luo, Y. Q. Chen, Fractional order proportional integral (FOPI) and [proportional integral] (FO[PI]) controller designs for first order plus time delay (FOPTD) systems, in: Control and Decision Conference, 2009. CCDC '09. Chinese, 2009, pp. 329–334.

[23] Y. Luo, Y. Q. Chen, Stabilizing and robust FOPI controller synthesis for first order plus time delay systems, in: Decision and Control and European Control Conference (CDC-ECC), 2011 50th IEEE Conference on, 2011, pp. 2040–2045.

[24] S. Das, S. Das, A. Gupta, Fractional order modeling of a PHWR under step-back condition and control of its global power with a robust controller, IEEE Transactions on Nuclear Science 58 (5) (2011) 2431–2441.

[25] K. Sundaravadivu, B. Arun, K. Saravanan, Design of fractional order PID controller for liquid level control of spherical tank, in: Control System, Computing and Engineering (ICCSCE), 2011 IEEE International Conference on, 2011, pp. 291–295.

[26] A. Tepljakov, E. Petlenkov, J. Belikov, FOMCON: a MATLAB toolbox for fractional-order system identification and control, International Journal of Microelectronics and Computer Science 2 (2) (2011) 51–62.

[27] A. Tepljakov, E. Petlenkov, J. Belikov, FOMCON toolbox (2011).
URL `http://www.fomcon.net/`

[28] D. Xue, Y. Q. Chen, D. P. Atherton, Linear Feedback Control: Analysis and Design with MATLAB (Advances in Design and Control), 1st Edition, Society for Industrial and Applied Mathematics, Philadelphia, PA, USA, 2008.

[29] A. Tepljakov, E. Petlenkov, J. Belikov, J. Finajev, Fractional-order controller design and digital implementation using FOMCON toolbox for MATLAB, in: Proc. of the 2013 IEEE Multi-Conference on Systems and Control conference, 2013, pp. 340–345.

[30] K. Åström, T. Hägglund, PID Controllers: Theory, Design, and Tuning, 2nd Edition, The Instrumentation, Systems, and Automation Society (ISA), 1995.

[31] C. A. Monje, B. M. Vinagre, V. Feliu, Y. Q. Chen, Tuning and auto-tuning of fractional order controllers for industry applications, Control Engineering Practice 16 (7) (2008) 798–812.

[32] M. Goldfarb, T. Sirithanapipat, The effect of actuator saturation on the performance of PD-controlled servo systems, Mechatronics 9 (5) (1999) 497–511.

[33] Official website of INTECO, LLC., [Last access time: 05.11.2014] (2013).
URL `http://www.inteco.com.pl/`

[34] A. Tepljakov, E. Petlenkov, J. Belikov, S. Astapov, Digital fractional-order control of a position servo, in: Proc. 20th Int Mixed Design of Integrated Circuits and Systems (MIXDES) Conference, 2013, pp. 462–467.

[35] J. G. Ziegler, N. B. Nichols, Optimum settings for automatic controllers, in: Transactions of the A.S.M.E., 1942, pp. 759–768.

[36] A. O'Dwyer, Handbook of PI and PID Controller Tunning Rules, 3rd Edition, Imperial College Press, 2009.